Supplementary Information

Description of Study Sites

Situated at the western end of the Taylor Glacier, Beacon Valley (BV, 77º48' S, 160º48' E) contains the oldest glacial ice on Earth (Schäfer et al. 2000). The ice layer, primarily localized to central Beacon Valley, rests below a 50 cm thick sublimation till composed of clasts of Ferrar Dolerite, Beacon Sandstone, and granite erratics foreign to Beacon Valley (Kowalewski et al. 2006). There is very limited sublimation from the buried glacial ice even during the austral summer (Kowalewski et al. 2006). The average air relative humidity (RH) content in the austral summer is around 35%, and the air temperature ranges from -16ºC to 3.3ºC, although ground-surface temperature can be 5-10ºC higher (Kowalewski et al. 2006). These factors, in combination with Beacon Valley's high elevations (alt. ~1500 m) and exposure to katabatic winds coming from the nearby Polar Plateau, suggest extremely limited water availability for microorganisms. The sampling site, situated at the center of a very large sublimation polygon, is typical of the soil described above.

Battleship Promontory (BP, 76º54' S, 160º55' E) in the Convoy Range is by far the northern-most study site included in the study. Summer average relative humidity is around 54%, and rock surface temperature ranges from -14.2ºC to 9.9ºC (Wynn-Williams 2000). Battleship Promontory has long been considered a "hot spot" for endolithic life (Banerjee et al. 2000) and is thought to harbor considerable free-living cyanobacteria populations (Johnston & Vestal 1991; Wynn-Williams & Edwards 2000). Despite the relatively high altitude, transient ponds formed from snow melt water are frequently observed at Battleship Promontory. The sampling site, covering several sublimation polygons, is composed of weathered Beacon Sandstone beneath a layer of Ferrar Dolerite pebbles.

Upper Wright Valley (UW, 77º10' S, 161º50' E) is defined as the areas between

Wright Upper Glacier and Lake Vanda and comprises three distinct areas: the Labyrinth, the Dais, and the North and South forks bifurcated by the Dais (McLeod et al. 2009). The underlying geology of the area is Ferrar Dolerite and Beacon Sandstone, which are clearly visible along the sides of the valley. Air relative humidity and temperature are considered to be too low to produce significant soil moisture, and saltpans are a common occurrence in the area (McLeod et al. 2009). The sampling site is located in an elevated area north of the boundary between Wright Upper Glacier and the Labyrinth, where the soil is a mixture of Ferrar Dolerite and Beacon Sandstone derived from glacial till. The soil is likely to be relatively old due to the presence of locally weathered boulders and finely weathered surface material.

Miers Valley (MV, 78º60' S, 164º00' E) is the southern-most and the only coastal valley (alt. ~150 m) included in the study. Its predominant underlying geology is marble and granite, although most of the valley floor is covered by moraine of glacial and/or marine origin, as is typical of the eastern Dry Valleys (Bockheim & McLeod 2008). Due to its coastal location and low altitude, Miers Valley has higher precipitation than other valleys, and during the austral summer, glacial melt streams from Miers and Adams glaciers become highly active and form a hyporheic zone west of the Miers Lake. The sampling site is west of the Miers Lake and at least 250 m north of the clearly defined hyporheic zone, in an area dominated by moraine with very few large boulders.

Detailed DNA Extraction Protocol

0.8 g of soil was placed into a screw-cap microcentrifuge tube containing 0.1 mm and 2.5 mm silica-zirconia beads (0.5 g each) (BioSpec Products, Bartlesville, Oklahoma). 300 µl of phosphate buffer (100 mM NaH_2PO_4) and 300 µl of SDS lysis buffer (100 mM NaCl, 500 mM Tris pH 8.0, and 10% SDS) were added to the tube, and the tube was shaken at 4.2 ms^{-1}

for 30 seconds on a MiniBeadBeater (Glen Mills Inc, Clifton, New Jersey). After centrifugation at 16,000 x g for 3 minutes, the aqueous phase was transferred to a new tube, and 200 µl of cetyltrimethylammonium bromide (CTAB) extraction buffer (100 mM Tris·HCl pH 8.0, 1.4 M NaCl, 25 mM EDTA, 2% hexadecyltrimethylammonium bromide, 1% polyvinylpyrrolidone, 0.4% v/v beta-mercaptoethanol) was added, followed by incubation at 60ºC for 30 minutes. After centrifugation at 16,000 x g for 5 minutes, the aqueous phase (transferred to a new tube) was mixed with equal volume of chloroform:isoamyl alcohol (24:1) and incubated on a platform rocker at room temperature for 20 minutes. After centrifugation at 16,000 x g for 5 minutes, 7 M ammonium acetate was added to the aqueous phase in a new tube to a final concentration of 2.5 M, and the tube was centrifuged again at 16,000 x g for 5 minutes. The supernatant was transferred to a new tube, and 0.54 volumes of ice-cold isopropanol was added. After overnight incubation at -20ºC, the precipitated DNA was centrifuged at 16,000 x g for 20 minutes, washed with ice-cold 70% ethanol, and air dried. The recovered DNA was resuspended in 20 µl TE buffer and quantified using a NanoDrop 1000 spectrophotometer (NanoDrop Products, Wilmington, Delaware). Procedural blanks were included at appropriate steps and yielded no DNA detectable by PCR.

PCR Components and Conditions and Quality Control Procedure for Community Fingerprinting Analysis

Duplicate PCR of 50 µl was performed with 10 to 50 ng of template DNA per tube. The PCR components included: 1X Platinum *Taq* PCR buffer, 0.2 mM dNTPs, 20 µg/ml bovine serum albumin (BSA), 3 mM $MgCl_2$, 1 unit of Platinum *Taq* (Invitrogen Inc., Carlsbad, California), 300 nM of each primer, and de-ionized water. All PCR runs were performed on a Bio-Rad DNA Engine (PTC-200, Bio-Rad Laboratories Inc, Hercules,

California), and the thermocycler program was as follows: 94ºC for 2 minutes, followed by 30/35 cycles (bacterial/cyanobacterial ARISA) of 94ºC for 45 seconds, 55ºC for 30 seconds, 72ºC for 2 minutes, and a final extension at 72ºC for 7 minutes. Duplicate PCR products were combined and visualized on 1% agarose gel, then cleaned up using a QuickClean PCR Purification kit (GenScript Corporation, Piscataway, New Jersey). PCR amplicons were quantified using a NanoDrop 1000 spectrophotometer (NanoDrop Products, Wilmington, Delaware) and diluted 1:10 using de-ionized water.

Soil Sample Preparation for Elemental Analysis (ICP-MS)

4 ml of concentrated HNO_3 (first diluted 1:1 using de-ionized water) and 10 ml of concentrated HCl (first diluted 1:4 using de-ionized water) were added to 1 g of soil in a covered beaker and incubated at room temperature for 30 minutes. The samples were then digested at 95ºC for 30 minutes, cooled, and diluted to a final volume of 100 ml. Sub-samples (approx. 30 ml) were transferred to 50 ml Falcon tubes and centrifuged at 800 x g for 10 minutes. 1.6 ml of concentrated HNO_3 was added to 20 ml of supernatant and consequently diluted to a final volume of 100 ml, an aliquot of which was then filtered through a 0.45 µl filter into a 15 ml Falcon tube. The resulting samples were analyzed using an ELAN DRC II mass spectrometer (Perkin-Elmer Inc., Münster, Germany). A procedural blank containing no soil returned negligible readings.

PCR Components and Conditions and Quality Control Procedure for Pyrosequencing of PCR Amplicons

For each study site, triplicates of 30 µl PCR with 15 or 30 ng of pooled genomic DNA template per tube were used to reduce the effects of stochastic PCR bias (Wintzingerode et al. 1997). The PCR components included: 1X PrimerSTAR Buffer (includes 1 mM Mg^{2+}), 0.2

mM dNTPs, 5 units of PrimeSTAR HD DNA Polymerase (Takara Bio Inc., Shiga, Japan), 400 nM of each primer, and de-ionized water. All PCR runs were performed on a Bio-Rad DNA Engine (Bio-Rad Laboratories Inc.), and the thermocycler program was as follows: 94ºC for 2 minutes, followed by 30 cycles of 94ºC for 20 seconds, 55ºC (decrease 0.2 per cycle) for 10 seconds, 72ºC for 20 seconds, and a final extension at 72ºC for 3 minutes. Triplicate PCR products were combined and run on a 2% agarose gel, which was stained with SYBR Gold Nucleic Acid Gel Stain (Invitrogen Inc.) and visualized on a Safe Imager Blue-Light Transilluminator (Invitrogen Inc.) to avoid UV-related damage to the amplicons. DNA bands of the correct size were extracted from the agarose gel and purified using a QuickClean Gel Extraction kit (GenScript Corporation). The resulting PCR amplicons were quantified using both a NanoDrop 1000 spectrophotometer and a QuBit Fluorometer (Invitrogen Inc.).

Noise-Filtering and Binning of ARISA Run Data

ARISA run data were processed using Genetic Profiler (Version 2, GE Healthcare) to yield all detectable peaks without applying any arbitrary cutoff. The resulting data was processed using a modified version of a previously described program (Abdo et al. 2006), which defined the background noise baseline through recursive analysis, and peaks within 6 S.D. of the noise baseline were removed. The remaining peaks were binned to counter size variance between ARISA runs. ARISA results from procedural blanks were used to remove background signals due to contamination or noise. For the FAM-labeled cyanobacterial ARISA samples, potential crosstalk AFLs from the ROX-labeled size standards were manually removed based on known ETR900-R sizes. All AFLs smaller than 120 bp for bacterial ARISA and 180 bp for cyanobacterial ARISA were removed since they were too short to contain true ITS regions (Wood et al. 2008).

Abdo Z, Schütte UME, Bent SJ, Williams CJ, Forney LJ, Joyce P. (2006). Statistical methods for characterizing diversity of microbial communities by analysis of terminal restriction fragment length polymorphisms of 16S rRNA genes. Environ Microbiol 8:929–938.

Banerjee M, Whitton BA, Wynn-Williams DD. (2000). Phosphatase Activities of Endolithic Communities in Rocks of the Antarctic Dry Valleys. Microb Ecol 39:80–91.

Bockheim JG, McLeod M. (2008). Soil distribution in the McMurdo Dry Valleys, Antarctica. Geoderma 144:43–49.

Johnston C, Vestal J. (1991). Photosynthetic carbon incorporation and turnover in Antarctic cryptoendolithic microbial communities: are they the slowest-growing communities on Earth? Appl Environ Microbiol 57:2308–2311.

Kowalewski, Marchant D, Levy, Head JW. (2006). Quantifying low rates of summertime sublimation for buried glacier ice in Beacon Valley, Antarctica. Antarct Sci 18:421–428.

McLeod M, Bockheim JG, Balks M, Aislabie J. (2009). Soils of western Wright Valley, Antarctica. Antarct Sci 21:355–365.

Schäfer J, Baur H, Denton G, Ivy-Ochs S, Marchant D, Schlüchter C, et al. (2000). The oldest ice on Earth in Beacon Valley, Antarctica: new evidence from surface exposure dating. Earth Planet Sc Lett 179:91–99.

Wintzingerode von F, Göbel U, Stackebrandt E. (1997). Determination of microbial diversity in environmental samples: pitfalls of PCR-based rRNA analysis. FEMS Microbiol Rev 21:213–229.

Wood SA, Rueckert A, Cowan D, Cary SC. (2008). Sources of edaphic cyanobacterial diversity in the Dry Valleys of Eastern Antarctica. ISME J 2:308–320.

Wynn-Williams DD. (2000). Cyanobacteria in deserts. In:The Ecology of Cyanobacteria, Whitton, BA & Potts, M, eds (ed). Kluwer Academic Publishers: Dordrecht, Netherlands, pp. 341–366.

Wynn-Williams DD, Edwards, HGM. (2000). Antarctic ecosystems as models for extraterrestrial surface habitats. Planet Space Sci 48:1065–1075.

Supplementary Figure 1: Comparison of Observed and Predicted Diversities from Multiple Sequence Alignment Algorithms

Non-redundant high quality reads were aligned using ClustalW, PRANK$_{+F}$, and NAST. The numbers of raw reads are represented by white bars, numbers of observed OTUs$_{0.03}$ by black bars, ChaoI indices for OTUs$_{0.03}$ by light gray bars, and ACE indices for OTUs$_{0.03}$ by dark gray bars. Error bars correspond to standard errors for the alpha diversity indices.

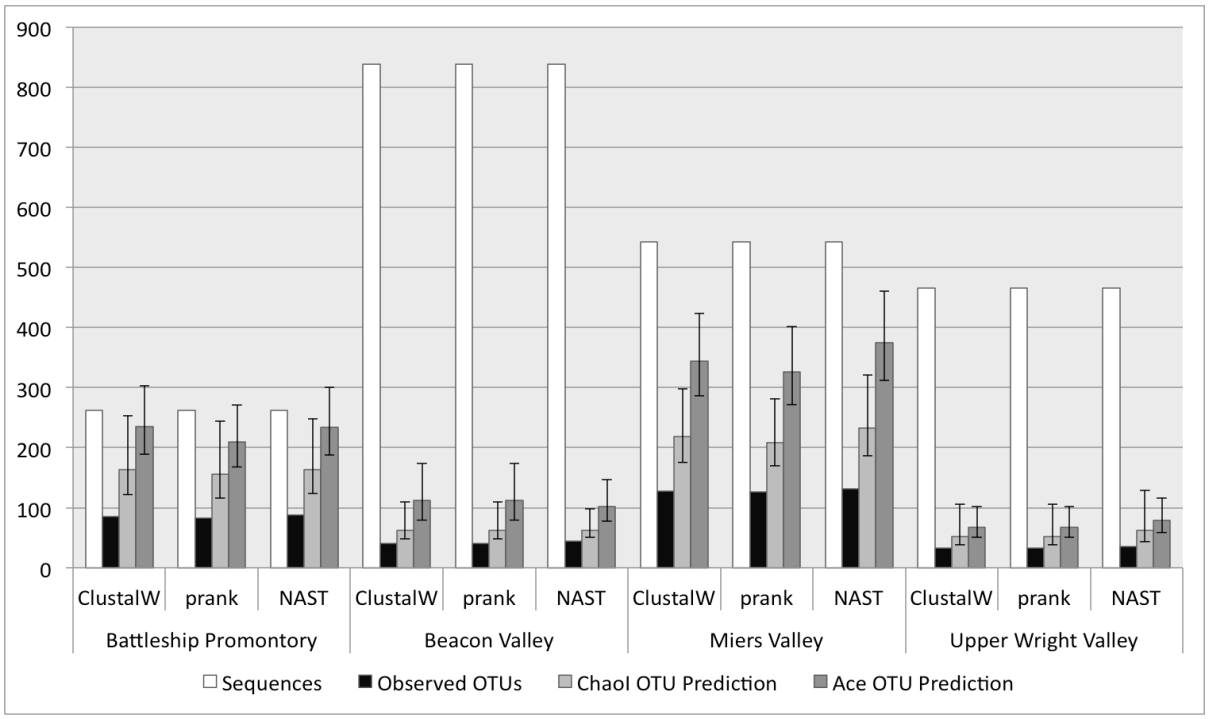

Supplementary Figure 2: Rarefaction Curves for $OTUs_{0.03}$

The rarefaction curves for $OTUs_{0.03}$ observed in the four study sites are as follows: Miers Valley, light gray triangles; Battleship Promontory, dark gray diamonds; Beacon Valley, light gray squares; Upper Wright Valley, light gray crosses.

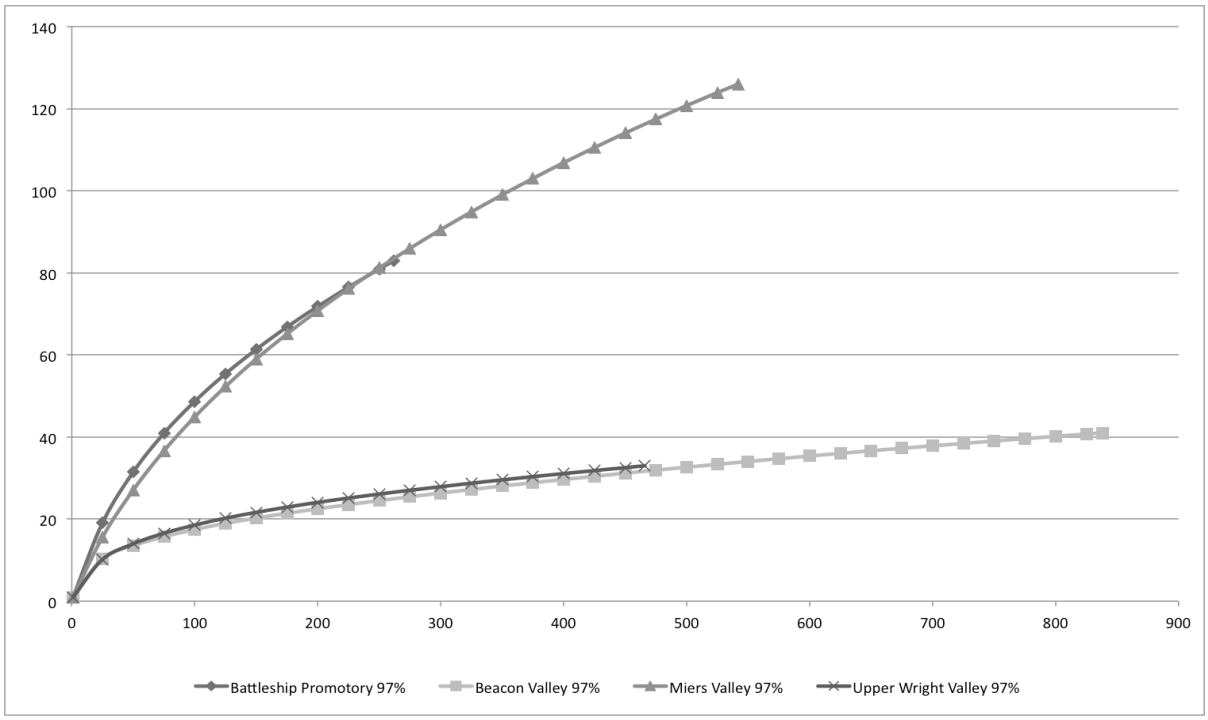

Supplementary Figure 3: Rank-Abundance Distributions of $OTUs_{0.03}$

The X axis ranks all $OTUs_{0.03}$ in order of abundance, and the Y axis represents the number of sequences in each $OTU_{0.03}$. Both axes are in logarithmic scale. The study sites are represented using the following symbols: Miers Valley, green triangles; Battleship Promontory, blue diamonds; Beacon Valley, red squares; Upper Wright Valley, purple crosses.

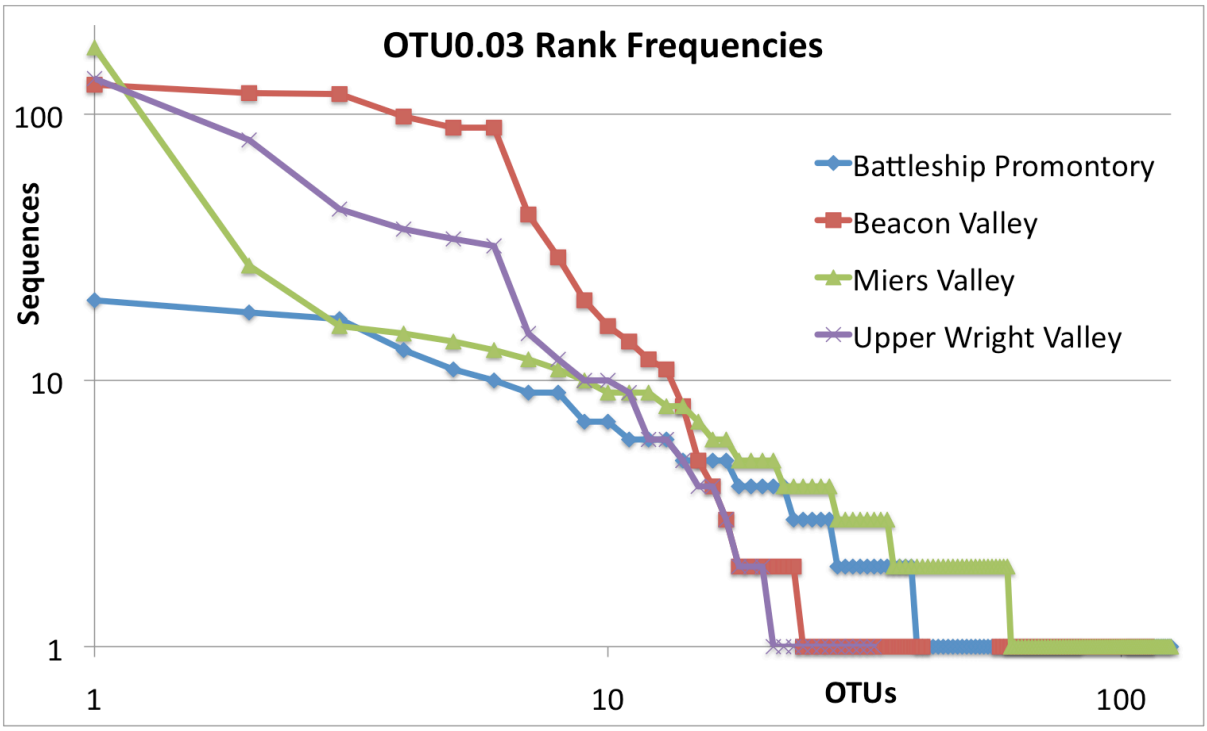

Supplementary Figure 4: LINKTREE Analysis of Bacteria (A) and Cyanobacterial (B) ARISA Patterns in Conjunction with Physicochemical Parameters

The LINKTREE analysis binary-splits the samples successively using a single most divisive environmental variable (although multiple variables may be equally divisive), which are listed in Supplementary Table 6. Samples within each group that cannot be split further (i.e., *p* value greater than 0.05) are thus biologically and physicochemically similar. ARISA samples are presented as numbers in the trees: samples #1 through #5, MV_A through MV-X; samples #6 through #10, BV_A through BV_X; samples #11 through #15: BP_A through BP_X; samples #16 through #20: UW_A through UW-X.

A	B

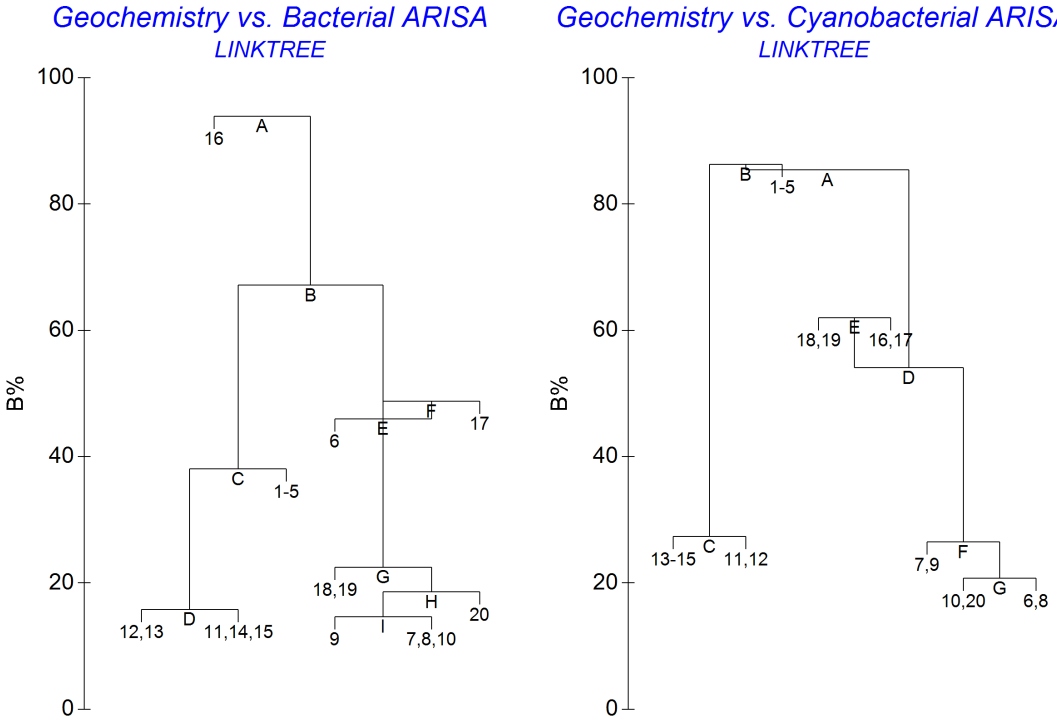

Supplementary Table 1: ANOSIM Analysis of Soil Geochemical Properties

Pairwise R-values for all geochemical properties shown in Table 1 are listed in the lower triangular, and pairwise R-values for ICP/MS values are listed in the upper triangular and in parentheses. p-values for all pairs are 0.008.

200

	Beacon Valley	Upper Wright Valley	Battleship Promontory	Miers Valley
Beacon Valley	X	(0.524)	(0.524)	(0.812)
Upper Wright Valley	0.564	X	(0.712)	(0.94)
Battleship Promontory	0.672	0.856	X	(0.96)
Miers Valley	0.956	0.996	0.98	X

Supplementary Table 2: Complete Soil Geochemical Properties

(Element concentrations in ppb)	MV_A	MV_B	MV_C	MV_D	MV_X	BV_A	BV_B	BV_C	BV_D	BV_X
pH	8.9	8.8	8.1	8.6	8.7	6.9	7	7	7	7.6
Conductivity (µS)	300	300	300	300	300	3920	3920	3920	3920	3920
Gravimetric Water Content (%)	0.53%		0.52%			2.25%		2.47%		
% C	0.27	0.46	0.47	0.41	0.70	0.11	0.20	0.17	0.11	0.11
% N	0.01	0.05	0.05	0.06	0.06	0.06	0.08	0.09	0.08	0.08
C/N	54.00	9.20	9.40	6.83	11.67	1.83	2.50	1.89	1.38	1.38
Li	18.92	11.95	15.63	20.04	18.96	12.55	10.59	20.31	12.67	14.47
B	1029.13	1080.90	1012.14	974.69	956.64	944.42	1010.81	1075.94	975.18	1062.91
Na	7615.44	5886.48	7362.35	9681.16	8291.59	3316.58	3219.94	6827.89	4354.56	4414.27
Mg	42724.53	29478.33	41811.32	48057.06	41376.36	9136.12	9283.76	14285.56	9670.57	10429.54
Al	24602.74	16071.96	22145.90	29281.29	25104.35	24230.63	18844.32	38396.40	25558.47	29333.16
Si	13739.24	9046.16	12929.20	17651.65	8573.35	2002.72	1913.98	1857.00	1858.11	1799.48
P	1314.75	1573.20	1724.62	2169.05	1971.41	1008.13	1237.78	1000.76	782.91	842.45
K	5375.36	3539.77	4525.19	6395.32	5950.87	1291.35	1349.68	3466.62	2095.38	2290.63
Ca	24663.46	16804.91	23436.45	30856.43	27604.81	17984.44	9099.23	21134.72	16395.50	16322.57
Ti	5674.47	3418.16	4754.81	6794.96	4918.48	842.92	356.82	1242.88	718.32	1008.47
V	78.49	54.80	76.50	98.62	83.52	122.37	82.77	215.15	148.25	210.56
Cr	53.31	36.87	55.93	64.10	48.99	8.66	6.94	16.36	11.02	11.85
Fe	45971.43	30961.85	43262.72	54330.99	47124.06	41521.27	40086.20	66271.29	43673.53	52303.92
Mn	742.19	518.72	727.17	892.11	787.33	417.19	323.34	584.29	379.91	421.56
Co	31.90	20.95	32.17	37.47	31.91	20.82	20.71	27.73	20.39	22.04
Ni	174.81	117.41	185.82	200.45	169.66	24.43	24.86	38.26	27.67	29.87
Cu	24.78	15.22	23.47	29.92	26.06	123.12	149.88	188.97	134.87	139.79
Zn	114.51	96.34	103.57	100.23	107.56	92.69	79.44	137.74	99.19	111.59
As	0.87	1.20	1.30	4.38	1.54	2.19	1.70	3.00	1.91	2.19
Hf	0.87	0.34	0.58	0.73	0.52	0.41	0.25	0.63	0.31	0.40
Se	0.62	0.91	1.06	1.33	0.88	1.20	1.31	1.95	1.41	2.03
Sr	328.09	196.06	299.73	415.31	366.36	60.07	41.93	94.54	74.76	80.94
Zr	35.65	16.32	29.68	41.96	30.11	14.68	8.16	22.60	12.43	14.40
Ag	0.03	0.00	0.00	0.10	0.00	0.00	0.00	0.14	0.03	0.05
Cd	0.29	0.18	0.23	0.29	0.27	0.13	0.14	0.31	0.25	0.20
In	0.04	0.02	0.02	0.04	0.03	0.02	0.01	0.04	0.02	0.03
Ba	150.30	95.38	133.86	200.44	172.51	26.18	19.65	115.24	73.71	40.06
Hg	0.06	0.04	0.03	0.05	0.03	0.03	0.03	0.10	0.04	0.04
Tl	0.10	0.04	0.07	0.11	0.11	0.04	0.05	0.11	0.09	0.08

Pb	3.80	2.60	3.77	5.84	5.07	7.27	7.12	11.99	8.69	9.16
Bi	0.14	0.02	0.05	0.11	4.42	0.06	0.05	0.10	0.10	0.08
U	1.01	0.85	1.04	1.56	1.37	1.01	0.96	1.42	0.96	1.12

205

(Element concentrations in ppb)	BP_A	BP_B	BP_C	BP_D	BP_X	UW_A	UW_B	UW_C	UW_D	UW_X
pH	7.9	7.7	7.2	7.2	8.4	6.9	7.1	7	6.9	6.9
Conductivity (µS)	107	107	107	107	107	6130	6130	6130	6130	6130
Gravimetric Water Content (%)		1.17%		1.10%			1.05%		1.10%	
% C	0.10	0.10	0.09	0.10	0.10	0.10	0.11	0.13	0.11	0.10
% N	0.04	0.05	0.04	0.05	0.04	0.15	0.09	0.11	0.13	0.10
C/N	2.50	2.00	2.25	2.00	2.50	0.67	1.22	1.18	0.85	1.00
Li	10.28	7.37	7.56	7.87	8.62	12.70	13.13	9.82	15.23	16.01
B	1011.43	1066.09	1096.96	1014.18	1000.37	976.82	1060.32	1032.47	1043.78	1028.77
Na	3513.85	2709.95	2446.86	2831.78	2494.66	6920.16	4318.82	3800.44	7395.78	12718.43
Mg	6629.99	5155.96	4618.98	5494.16	5721.86	9631.34	7680.43	6344.37	8952.06	6800.97
Al	29820.62	23813.09	23162.74	24991.45	21661.85	19038.46	18678.92	13653.22	21619.86	27174.52
Si	1895.41	1797.64	1855.81	1610.42	1654.85	1534.66	2075.08	1851.26	2044.63	1938.68
P	892.97	744.50	616.47	620.59	722.81	636.18	593.10	370.90	503.58	483.16
K	1234.61	922.62	915.68	979.78	1077.94	2472.14	2700.96	2252.89	4000.77	7336.59
Ca	11552.11	10078.24	8940.83	9862.03	8631.41	5504.80	5041.14	2944.20	5521.00	8458.98
Ti	921.21	808.58	764.65	953.06	861.24	599.48	508.61	360.81	439.76	396.18
V	88.56	73.98	72.46	92.64	75.95	71.44	82.30	53.30	58.99	56.94
Cr	8.63	7.38	7.15	7.13	6.99	8.61	9.59	6.91	10.36	7.60
Fe	37354.94	30446.37	27730.78	30070.54	34114.71	29648.20	31110.01	21054.85	29985.89	26991.41
Mn	358.64	291.03	257.07	315.41	364.96	271.77	283.09	191.07	314.40	442.49
Co	19.59	14.95	13.05	15.60	17.39	14.79	14.31	9.51	13.61	10.41
Ni	27.75	22.05	19.16	22.34	21.27	19.82	19.75	14.50	20.30	16.39
Cu	121.75	96.28	77.57	98.08	104.83	78.02	73.48	52.64	70.78	55.87
Zn	68.52	57.30	49.62	68.56	72.41	65.35	73.76	48.12	69.05	66.79
As	1.40	1.28	0.69	1.13	1.33	1.95	1.77	2.16	2.18	1.71
Hf	0.33	0.27	0.20	0.28	0.31	0.31	0.38	0.29	0.45	0.51
Se	1.12	1.06	0.97	1.56	1.08	1.38	1.01	1.02	1.08	1.15
Sr	44.54	36.53	32.90	38.96	33.14	34.68	28.93	20.79	36.80	40.93
Zr	10.99	9.94	6.67	11.60	11.47	13.36	13.47	12.02	24.38	26.85
Ag	0.00	0.00	0.00	0.00	0.00	0.01	0.00	0.00	0.00	0.00
Cd	0.15	0.08	0.11	0.17	0.16	0.30	0.12	0.10	0.13	0.20
In	0.02	0.01	0.02	0.02	0.02	0.01	0.02	0.01	0.02	0.02
Ba	28.27	21.91	19.31	27.99	25.76	42.41	36.89	28.75	42.73	49.54
Hg	0.02	0.01	0.01	0.02	0.02	0.03	0.01	0.01	0.02	0.04
Tl	0.05	0.01	0.03	0.03	0.04	0.09	0.07	0.04	0.09	0.12
Pb	4.31	3.24	3.03	3.64	3.88	9.07	8.78	6.69	11.45	9.70

Bi	0.03	0.01	0.01	0.02	0.02	0.04	0.06	0.04	0.06	0.07
U	1.10	0.85	0.78	0.87	0.87	0.83	0.91	0.60	1.12	1.79

Supplementary Table 3: Numbers of ARISA Fragment Length Groups (AFLs) Identified in Bacterial and Cyanobacterial Profiles

	Total Bacterial AFL	Average Bacterial AFL±S.D.	Total Cyanobacterial AFL	Average Cyanobacterial AFL±S.D.
Beacon Valley	83	16.6±4.0	43	8.6±2.9
Upper Wright Valley	98	19.6±8.7	24	4.8±1.3
Battleship Promontory	177	35.4±9.4	31	6.2±4.0
Miers Valley	174	34.8±5.1	56	11.2±4.2

Supplementary Table 4: ANOSIM Analysis of Bacterial and Cyanobacterial ARISA Profiles

Pairwise R-values for bacterial ARISA profiles are listed in the lower triangular, and pairwise R-values for cyanobacterial ARISA profiles are listed in the upper triangular and in parentheses. p-values for all pairs are 0.008, except for the BV-UW pair (0.024 for bacterial ARISA and 0.103 for cyanobacterial ARISA)

	Beacon Valley	Upper Wright Valley	Battleship Promontory	Miers Valley
Beacon Valley	X	(0.216)	(1)	(0.998)
Upper Wright Valley	0.214	X	(0.594)	(0.752)
Battleship Promontory	0.958	0.596	X	(0.99)
Miers Valley	0.974	0.616	0.952	X

Supplementary Table 5: Biogeochemical Analysis

The Biota-Envionrmental STepwise (BEST) analysis was carried out to investigate potential links between physicochemical parameters (up to five) and ARISA patterns (both bacterial and cyanobacterial ARISA). p-values for both BEST analyses are 0.01. A Rho value (aka Spearman's rank correlation coefficient) of 1 indicates perfect correlation, and 0 no correlation.

Geochem vs. Bacterial ARISA		Geochem vs. Cyanobacterial ARISA	
Rho	Variables	Rho	Variables
0.567	Altitude, µS[1]	0.622	Altitude, µS, Cu
0.560	Altitude, µS, %N, Pb	0.623	Altitude, µS, Cu, Ni
0.560	µS, pH, Ca, Pb	0.623	Altitude, µS, W_G[2], Cu
0.563	Altitude, µS, pH, Pb, B	0.623	Altitude, µS, W_G[2], Cu, Ni
0.560	Altitude, µS, pH, Pb, Ca	0.621	Altitude, µS, Cu, Ni, Si

[1]conductivity; [2]gravimetric water content.

Supplementary Table 6: Environmental Variables Corresponding to LINKTREE Splits

Environmental variables that facilitate successful binary splits (i.e., p-value <0.05) in LINKTREE analysis (Supplementary Figure 4) are listed here. The soil physicochemical values shown here been transformed and normalized as described in Material and methods and can only be interpreted in relative terms. Nodes and samples are represented using the same scheme as Supplementary Figure 4.

Node->Split	Variable	LHS[1] (RHS)[2] Split	π[3]	*p* value	R[4]	B%[5]
Bacterial ARISA (Supplementary Figure 4A)						
A->(16), B	%N	>1.77 (<1.43)	1.92	0.001	0.87	93.9%
	C/N	<-1.08 (>-0.93)				
	Si	<-0.765 (>-0.709)				
	W_G	<-0.662 (>-0.64)				
B->C, E	µS	<-0.664 (>0.818)	1.9	0.001	0.83	67.1%
	Pb	<-2.39E-2 (>0.265)				
C->D, (1-5)	W_G	<-0.623 (>1.68)	2.58	0.001	0.95	38%
	Altitude	>0.421 (<-1.65)				
	Mg	<-0.704 (>1.19)				
	Si	<-0.518 (>1.26)				
	Cr	<-0.558 (>1.2)				
	Ni	<-0.336 (>1.24)				
	Ba	<-0.738 (>0.821)				
	Sr	<-0.489 (>1.06)				
	K	<-0.97 (>0.549)				
	%C	<-0.675 (>0.68)				
	Ti	<-0.16 (>1.17)				
	Cu	>0.157 (<-1.15)				
	Na	<-0.681 (>0.37)				
	Zn	<-0.387 (>0.6)				
	C/N	<-0.128 (>0.784)				
	Mn	<-0.264 (>0.573)				
	P	<2.46E-2 (>0.815)				
	Zr	<-0.658 (>-2.87E-3)				
	Ca	<-3.03E-2 (>0.558)				
	µS	<-1.23 (>-0.664)				
	Li	<-0.644 (>-0.184)				
	Hg	<-0.253 (>0.186)				
	Co	<5.2E-2 (>0.227)				
	Cd	<-0.228 (>-9.61E-2)				
	Hf	<-0.469 (>-0.375)				
D->(12,13), (11,14,15)	B	>1 (<-0.178)	0.31	0.005	0.58	15.8%
	Cd	<-1.27 (>-0.441)				
	Zn	<-1.19 (>-0.577)				
	Hg	<-1.3 (>-0.787)				
	Pb	<-1.21 (>-0.978)				
	Ba	<-1.05 (>-0.853)				
	Mn	<-0.799 (>-0.61)				
	Zr	<-0.946 (>-0.758)				
	Li	<-1.56 (>-1.44)				
	Bi	<-0.653 (>-0.541)				
	U	<-0.721 (>-0.61)				
	Co	<-0.644 (>-0.536)				
	Se	<-0.388 (>-0.301)				
	K	<-1.39 (>-1.3)				
	Mg	<-1.02 (>-0.941)				

Node->Split	Variable	LHS[1] (RHS)[2] Split	π[3]	*p* value	R[4]	B%[5]
	Hf	<-0.938 (>-0.863)				
	V	<-0.421 (>-0.355)				
	Ti	<-0.329 (>-0.264)				
	Cu	<0.464 (>0.491)				
E->(6), F	B	<-1.86 (>-1.1)	1.23	0.001	0.68	46%
	%N	<-0.148 (>0.385)				
	Tl	<-0.791 (>-0.607)				
	K	<-0.906 (>-0.842)				
F->G, (17)	Se	>-0.502 (<-0.533)	1.34	0.001	0.82	48.8%
	Si	<-0.429 (>-0.412)				
G->(18,19), H	Ca	<-1.19 (>-0.519)	1.25	0.001	0.59	22.5%
	Hg	<-0.572 (>-0.137)				
	Se	<-0.294 (>-8.2E-2)				
	% N	>1.05 (<0.841)				
	Cd	<-0.77 (>-0.569)				
	Sr	<-0.679 (>-0.573)				
	Mn	<-0.617 (>-0.551)				
H->I, (20)	Co	>0.157 (<-1.55)	0.99	0.001	0.75	18.6%
	Fe	>0.306 (<-1.09)				
	Na	<0.672 (>1.94)				
	Cu	>0.95 (<-0.304)				
	K	<0.519 (>1.61)				
	U	<1.3 (>2.29)				
	P	>-0.243 (<-1.22)				
	V	>-0.14 (<-1.07)				
	Zn	>-6.83E-2 (<-0.664)				
	Altitude	>0.879 (<0.351)				
	Se	>0.397 (<-8.2E-2)				
	Ni	>-0.45 (<-0.872)				
	Mg	>-0.279 (<-0.672)				
	Zr	<0.643 (>0.992)				
	µS	<0.818 (>1.08)				
	C/N	>-0.595 (<-0.819)				
	%N	<0.621 (>0.841)				
	W_G	>-0.431 (<-0.623)				
	Tl	<1.18 (>1.36)				
	pH	>-0.809 (<-0.959)				
	Ca	>-0.404 (<-0.519)				
	%C	>-0.565 (<-0.675)				
	Sr	>-0.549 (<-0.573)				
	Si	<-0.507 (>-0.492)				
I->(9), (7,8,10)	B	<-1.1 (>-0.256)	1.22	0.001	1	14.6%
	P	<-0.243 (>-9.39E-2)				
	Cu	<0.95 (>1)				
	Co	<0.157 (>0.197)				
Cyanobacterial ARISA (Supplementary Figure 4B)						
A->B, D	µS	<-0.664 (>0.818)	1.91	0.001	0.54	85.4%
	Pb	<-2.39E-2 (>0.265)				
B->C, (1-5)	W_G	<-0.623 (>1.68)	2.58	0.001	0.99	86.3%
	Altitude	>0.421 (<-1.65)				
	Mg	<-0.704 (>1.19)				
	Si	<-0.518 (>1.26)				
	Cr	<-0.558 (>1.2)				
	Ni	<-0.336 (>1.24)				
	Ba	<-0.738 (>0.821)				
	Sr	<-0.489 (>1.06)				
	K	<-0.97 (>0.549)				
	%C	<-0.675 (>0.68)				
	Ti	<-0.16 (>1.17)				

Node->Split	Variable	LHS[1] (RHS)[2] Split	π[3]	*p* value	R[4]	B%[5]
	Cu	>0.157 (<-1.15)				
	Na	<-0.681 (>0.37)				
	Zn	<-0.387 (>0.6)				
	C/N	<-0.128 (>0.784)				
	Mn	<-0.264 (>0.573)				
	P	<2.46E-2 (>0.815)				
	Zr	<-0.658 (>-2.87E-3)				
	Ca	<-3.03E-2 (>0.558)				
	µS	<-1.23 (>-0.664)				
	Li	<-0.644 (>-0.184)				
	Hg	<-0.253 (>0.186)				
	Co	<5.2E-2 (>0.227)				
	Cd	<-0.228 (>-9.61E-2)				
	Hf	<-0.469 (>-0.375)				
C->(13-15), (11,12)	P	<-0.405 (>-0.345)	0.32	0.004	0.83	27.3%
	Cr	<-0.767 (>-0.732)				
	Ca	<-0.278 (>-0.244)				
D->E, F	Ca	<-1.19 (>-0.519)	1.2	0.001	0.49	54.1%
	Sr	<-0.679 (>-0.573)				
	Mn	<-0.617 (>-0.551)				
E->(18,19), (16,17)	V	<-0.981 (>-0.507)	0.44	0.012	1	62%
	P	<-1.14 (>-0.806)				
	As	>0.626 (<0.367)				
	Ti	<-0.952 (>-0.804)				
	Co	<-0.881 (>-0.754)				
	Cu	<2.76E-2 (>8.03E-2)				
F->(7,9), G	Hf	<-0.588 (>1.66E-2)	1.06	0.001	0.57	26.5%
	Zr	<-0.527 (>-0.245)				
	Mn	<-0.169 (>5.33E-2)				
	U	<-0.235 (>-5.75E-2)				
G->(10,20),(6,8)	P	<-9.39E-2 (>0.257)	0.8	0.001	1	20.7%
	C/N	<-0.595 (>-0.378)				
	Ca	<0.512 (>0.665)				

[1]LHS: Left-Half Split, properties of the group to the left of the node; [2]RHS: Right-Half Split, properties of the group to the right of the node; [3]π: the statistic π, which is defined as the absolute deviation of the real profile from the mean of all permuted profiles and constitutes the metric for formal hypothesis testing; [4]R: Spearman Rho value; [5]B%: an absolute measure of group differences. A lower value indicates similar samples.